AD/A-003 471

AIRCRAFT FUEL TANK VULNERABILITY TO HYDRAULIC RAM: MODIFICATION OF THE NORTHROP FINITE ELEMENT COMPUTER CODE BR-1 TO INCLUDE FLUID-STRUCTURE INTERACTION--THEORY AND USER'S MANUAL FOR BR-1HR

R. E. Ball

Naval Postgraduate School

Prepared for:

Air Force Flight Dynamics Laboratory

July 1974

SECURITY CLASSIFICATION OF THIS PAGE (When Data Entered)

REPORT DOCUMENTATION PAGE

READ INSTRUCTIONS BEFORE COMPLETING FORM

1. REPORT NUMBER: NPS-57Bp74071	2. GOVT ACCESSION NO.
3. RECIPIENT'S CATALOG NUMBER: AD/A-003471	
4. TITLE (and Subtitle): AIRCRAFT FUEL TANK VULNERABILITY TO HYDRAULIC RAM: MODIFICATION OF THE NORTHROP FINITE ELEMENT COMPUTER CODE BR-1 TO INCLUDE FLUID-STRUCTURE INTERACTION--THEORY AND USER's MANUAL FOR BR-1HR	5. TYPE OF REPORT & PERIOD COVERED: Final Report 1 July 1973 - 30 June 1974
	6. PERFORMING ORG. REPORT NUMBER
7. AUTHOR(s): R. E. BALL	8. CONTRACT OR GRANT NUMBER(s)
9. PERFORMING ORGANIZATION NAME AND ADDRESS: NAVAL POSTGRADUATE SCHOOL MONTEREY, CA 93940	10. PROGRAM ELEMENT, PROJECT, TASK AREA & WORK UNIT NUMBERS: FY 1456-74-00001
11. CONTROLLING OFFICE NAME AND ADDRESS: AIR FORCE FLIGHT DYNAMICS LABORATORY WRIGHT-PATTERSON AFB, OH 45433	12. REPORT DATE: July 1974
	13. NUMBER OF PAGES: 35
14. MONITORING AGENCY NAME & ADDRESS (if different from Controlling Office)	15. SECURITY CLASS. (of this report): UNCLASSIFIED
	15a. DECLASSIFICATION/DOWNGRADING SCHEDULE

16. DISTRIBUTION STATEMENT (of this Report)

Approved for public release; distribution unlimited.

17. DISTRIBUTION STATEMENT (of the abstract entered in Block 20, if different from Report)

Aircraft Survivability
Aircraft Vulnerability
Fuel Cells
Hydraulic Ram

18. SUPPLEMENTARY NOTES

19. KEY WORDS (Continue on reverse side if necessary and identify by block number)

20. ABSTRACT (Continue on reverse side if necessary and identify by block number)

The finite element digital computer code BR-1, developed by the Northrop Corporation, for predicting the effects of internal air blast on combat aircraft structures is modified to include the effects of compressible fluid-structure interaction. The true interaction phenomenon is approximated by the piston theory. The modification enables the code to be used to predict the structural response of aircraft fuel tanks subjected to penetrating bullets and fragments. It can also be used in many other

fluid-structure interaction problems. This report contains the theory, the modifications, and the additional instructions required to operate the modified code, called BR-1HR. The code is operational on the IBM 360/67 in FORTRAN IV, Level H.

NAVAL POSTGRADUATE SCHOOL

Monterey, California

Rear Admiral I. W. Linder, USN
Superintendent

Jack Borsting
Provost

The work reported herein was supported by the Air Force Flight Dynamics Laboratory, Wright-Patterson AFB, Ohio.

This report was prepared by:

R. E. BALL, Associate Professor
Department of Aeronautics

Approved by:

R. W. BELL, Chairman
Department of Aeronautics

Released by:

R. R. POSSUM
Dean of Research

TABLE OF CONTENTS

I. INTRODUCTION

A. Background

The Northrop Corporation, under Air Force funding, has developed a finite element digital computer code, called BR-1, for predicting the inelastic, large deflection, transient response of combat aircraft skin-rib-stringer structures when subjected to internal air blast loading. The finite elements considered are flat rectangular plates and beam stiffeners. The theory, user's manual and code listing are given in References 1 and 2. The Air Force Flight Dynamics Laboratory wanted the BR-1 code modified so that it could be used to predict the response of aircraft fuel tank walls when subjected to fluid pressures due to projectiles passing through the fuel in the tank. The intense pressure and momentum in the fuel due to the penetrating projectile is referred to as the hydraulic ram loading. This report describes the modifications to the IBM version of the BR-1 code to account for the fluid (fuel) - structure (tank wall) interaction that occurs when bullets and metal fragments penetrate into aircraft fuel tanks. The modified code is called BR-1HR. The interaction between the compressible fluid and the structure is approximated by the piston theory. The code can also be used for many other compressible fluid-structure interaction problems.

B. Piston Theory

The total nonlinear problem of the response of a tank containing a fluid and subjected to a high speed penetrating projectile is extremely complex and presently defies analytical treatment. In general, the

equations for the fluid stresses and motion are coupled to those for the wall stresses and motion due to the continuity at the fluid-structure interface (3). One procedure for approximating the fluid-structure interaction phenomenon is the piston theory (4). This theory has been in use since the early 1940's when it was applied to the study of the effect of underwater explosions on ship plates. It provides the correct solution to the one-dimensional propagation of stresses in an acoustic medium due to a moving boundary. Several recent studies have been made to determine its accuracy when applied to two dimensional fluid-structure interaction problems (4,5).

Application of the piston theory to the interaction problem allows the structure equations and fluid equations to be uncoupled. The response of the wall is computed using the conventional structural response equations, with the normal pressure on the wall p given by

$$p = p_o + \rho c\,(v_i - \dot{w}) \qquad (1)$$

where p_o and v_i are the incident pressure and velocity of the fluid at the wall respectively, ρ is the fluid density, c is the acoustic velocity in the fluid, and $\dot{w}$ is the wall velocity*. The pressure, p_o, and velocity, v_i, are the pressure and velocity that would exist in the fluid if the interface was not there, i.e., p_o and v_i do not contain any "local" reflected effects. However, effects on p_o and v_i due to earlier reflections from other walls and free surfaces should be considered. In other words, p_o and v_i are the loading components due to

*A dot above a variable denotes a derivative with respect to time.

the free field and the scattered effects. The loading component due to the wall velocity $\dot{w}$ is called the radiation pressure.

C. The NWC Hydraulic Ram Computer Code

In order to use the piston theory to compute the tank wall response, it is necessary to know the incident fluid pressure p_o and velocity v_i over the entire fluid-wall interface as a function of time. In conjunction with this project Lundstrom, at the Naval Weapons Center, has developed a digital computer code that predicts the fluid pressures and velocities p_o and v_i throughout a rectangular body of fluid due to a penetrating ballistic projectile. The model is based upon replacing the projectile by a line of sources whose strength is determined by an energy balance between the kinetic and potential energy of the fluid and the energy loss due to drag forces on the projectile. Reflections from the structure-fluid interface are accounted for by considering the fluid boundary to be either stress free or rigid*. An extensive series of tests were performed at the Naval Weapons Center to obtain detailed pressure measurements for a variety of projectiles under a wide range of impact conditions. This data allowed the selection of important parameters such as tumbling distance, jacket stripping, etc., to be entered into the code. A description of the code and the instructions for operation are given in Reference 7. This code provides the values for p_o and v_i at user specified locations over the structure-fluid interface for the time span of interest.

* A study of the one-dimensional reflection of step pressure waves from typical aircraft fuel tank walls indicates that the stress free surface provides the more accurate approximation (6)

II. MODIFICATION OF THE BR-1 CODE

A. Incorporation of the Piston Theory

The BR-1 code has an option for the user to input a time varying pressure on each panel element. In the piston theory this pressure is the $p_o + \rho c v_i$ of Eq. 1. The other contributor to the wall loading given by Eq. 1 is $\dot{w}$, the wall velocity. Since the BR-1 code does not include damping effects, it is necessary to add the damping term $\rho c \dot{w}$ to the equations of motion.

The BR-1 code solves the set of equations (Eqs. 1 and 2, Ref. 1)

$$[M]\{\ddot{q}^*\} = \{F\} - \{P\} - [H]\{q^*\} = \{C\} \tag{2}$$

for the vector of global nodal generalized displacements $\{q^*\}$ as a function of time. These generalized displacements define the motion of the walls. The vector $\{F\}$ consists of global generalized external and body forces at the nodes of the elements. The matrix $[M]$ is the mass matrix.

The wall pressure p given by Eq. 1 causes external forces at the nodes. The external generalized forces at the nodes of each element in the local coordinate system, $\{f\}$, is given by (Eq. A-47, Ref. 1)

$$\{f\} = \iint_{(Aout)} \left[N_B\right]^T \left\{T_o\right\} dA \tag{3}$$

where $\left[N_B\right]^T$ is the transpose of the matrix of shape functions $[N]$, evaluated at the surface of the element, Aout is the surface of the element, and $\{T_o\}$ is the vector of applied surface tractions and moments. The order of $\{T_o\}$ is a 5x1 vector. Due to the fluid pressure loading

$$\begin{Bmatrix} T_1 \\ T_2 \\ T_3 \end{Bmatrix} = \begin{Bmatrix} 0 \\ 0 \\ p \end{Bmatrix} \tag{4}$$

where the subscripts denote the coordinates, (T_3 is normal to the element), and p is given by Eq. 1. The fourth and fifth elements of $\{T_o\}$ correspond to applied moments per unit middle surface area of the element, and are zero here. The numerical intergration of Eq. 3 can be accomplished by Gaussian quadrature. However, the $\{f\}$ is obtained in the BR-1 code in a more approximate way by using a lumping approach at the nodes of the element, as is done for the mass matrix evaluation, in order to save computation time. Thus, according to Eq. B-92 of Ref. 1, the external force vector at the rth node of the nth element is given by

$$\{f_{nr}\} = \frac{(x_2-x_1)\,(y_2-y_1)n}{4}\ \frac{p_n}{D_{nr}}\ \begin{Bmatrix} \theta_2 \\ -\theta_1 \\ 1 \\ 0 \\ 0 \end{Bmatrix}_{nr} \tag{5}$$

where p_n is the magnitude of the pressure on the element*, and $D_{nr} = \sqrt{(1+\theta_1^2+\theta_2^2)}_{nr}$ where θ_1 and θ_2 are the fourth and fifth local generalized displacements at the rth node. They appear here because the pressure is defined in BR-1 as the pressure normal to the deformed surface. The quantities (x_2-x_1) and (y_1-y_2) are the dimensions of the rectangular element.

The pressure p_n in the piston theory is given by Eq. 1, i.e.

$$p_n = p_{on} + (\rho c)_n\, v_{in} - (\rho c)_n\, \dot{w}_{nr} \tag{6}$$

* The assumption is made in the programming of BR-1 that the pressure is uniform over each element. This is contrary to the theoretical presentation where the pressure is defined at each node point.

where

$$(\rho c)_n = \begin{cases} \rho c \text{ if the nth element is in contact with the fluid} \\ 0 \text{ if the nth element is not in contact with the fluid.} \end{cases}$$

The variables p_{on} and v_{in} can be determined from the NWC computer code for each element for the time span of interest prior to the computation of the wall response. This data is then input as the known external pressure. The variable $\dot{w}_{nr}$ is an unknown dependent variable and is part of $\{\dot{q}^*\}$. Hence, it must be incorporated into the equations of motion, Eq. 2.

The $\{f_{nr}\}$ due to $\dot{w}_{nr}$ is given by

$$\{f_{nr}\} = \frac{-\left(x_2-x_1\right)\left(y_2-y_1\right)_n}{4} \frac{(\rho c)_n \dot{w}_{nr}}{D_{nr}} \begin{Bmatrix} \theta \\ -\beta_{21} \\ 1 \\ 0 \\ 0 \end{Bmatrix}_{nr} \tag{7a}$$

The global force vector at the rth node, $\{F\}_r$, is related to $\{f_{nr}\}$ in the form

$$\{F\}_r = \sum_{n_r} [J_n]^T \{f_{n\alpha}\}_{\alpha \rightarrow r} \tag{7b}$$

where $[J_n]$ is the transformation matrix from the global coordinate system to the nth element local coordinate system, $\sum_{n_r}$ means a summation over all elements containing the node r, and $\alpha \rightarrow r$ means node α corresponds physically to node r. Since the wall velocity in Eq. 7a is given in terms of the local coordinates, it must be converted to global coordinates. Thus, according to Eqs. A-77 and B-3 of Reference 1,

$$\dot{w}_{nr} = \lfloor J_n^3 \rfloor \{\dot{q}^*\}_r \tag{8}$$

where $\lfloor J_n^3 \rfloor$ is the third row of $[J_n]$. Thus, the global external force vector at the rth node $\{F\}_r$ becomes

$$\{F\}_r = -\frac{1}{4} \sum_{n_r} (\rho c)_n [J_n]^T \frac{(x_2-x_1)(y_2-y_1)_n}{D_{nr}} [J_n^3] \{\dot{q}^*_r\} \begin{Bmatrix} \theta_2 \\ -\theta_1 \\ 1 \\ 0 \\ 0 \end{Bmatrix}_{nr} \quad (9)$$

Note that $\{F\}_r$ is nonlinear since $\dot{\theta}_1$ and $\dot{\theta}_2$ are part of $\{\dot{q}^*\}_r$. If the rotations θ_1 and θ_2 are neglected in the computation of $\{F\}_r$, i.e., if the pressure is not truly normal to the deformed surface, $\{F\}$ for the total R nodes of the structure can be given in the form

$$\{F\} = - [D] \{\dot{q}^*\} \quad (10a)$$

where

$$[D] = \begin{bmatrix} [D]_1 & & & 0 \\ & [D]_2 & & \\ & & \ddots & \\ 0 & & & [D]_R \end{bmatrix} \quad (10b)$$

and $[D]_r$ is a 6x6 matrix given by

$$[D]_r = \frac{1}{4} \sum_{n_r} (\rho c)_n (x_2-x_1) (y_2-y_1)_n [J_n]^T \lfloor J_n^3 \rfloor \quad (10c)$$

B. Method of Solution

The BR-1 code solves for $\{q^*\}$ at discrete points in time using the explicit finite difference scheme (Eq. A-109, Ref. 1)

$$\{\Delta q^*\}_{t_{i+1}} = \{\Delta q^*\}_{t_i} + \Delta t \{\dot{q}^*_I\}_{t_i} + (\Delta t)^2 \{\ddot{q}^*\}_{t_i} \tag{11}$$

where Δt is the time interval between two time points, i.e.

$$\Delta t = t_{i+1} - t_1$$

and

$$\{\Delta q^*\}_{t_{i+1}} = \{q^*\}_{t_{i+1}} - \{q^*\}_{t_i} \tag{12}$$

The acceleration $\{\ddot{q}^*\}_{t_i}$ is obtained from Eq. (2) in the form

$$\{\ddot{q}^*\}_{t_i} = [M]^{-1} \{C\}_{t_i} \tag{13}$$

The $\{\dot{q}^*_I\}$ are due to impulsive loads which are known in the blast loading problem. In the BR-1 code $\{F\}$, $\{P\}$, $\{q^*\}$ and $\{\dot{q}^*_I\}$ are known at time t_i. Hence, $\{\Delta q^*\}_{t_{i+1}}$ and $\{q^*\}_{t_{i+1}}$ can be determined using Eqs. 11-13. For our situation, $\{F\}_{t_i}$ contains $\{\dot{q}^*\}_{t_i}$, which is unknown. We could approximate $\{\dot{q}^*\}_{t_i}$ with the backward finite difference form

$$\{\dot{q}^*\}_{t_i} = \{\Delta q^*\}_{t_i} / \Delta t \tag{14}$$

If we do, then $\{\dot{q}^*\}_{t_i}$ becomes known at t_i, $\{F\}$, and hence $\{C\}$, can be determined at t_i, and the procedure used in BR-1 is directly applicable. On the other hand, if we express $\{\dot{q}^*\}_{t_i}$ in the central finite difference form

$$\{\dot{q}^*\}_{t_i} = \left(\{\Delta q^*\}_{t_{i+1}} - \{\Delta q^*\}_{t_i} \right) \Big/ (2\Delta t) \tag{15}$$

then $\{F\}_{t_i}$, and hence $\{C\}_{t_i}$, depends upon $\{\Delta q\}_{t_{i+1}}$. Consequently $\{\Delta q^*\}_{t_{i+1}}$ appears on both the left and right hand side of Eq. 11. This requires a new solution procedure. A detailed study of the accuracy and numerical stability of these two approacnes, and a third approach, when applied to a single degree of freedom, damped oscillator is presented in the Appendix. The approach where $\{\dot{q}^*\}$ is given by the central difference expression, Eq. 15, is the one selected based upon the accuracy and stability properties of this scheme. Its shown in the Appendix that the maximum value of Δt for a stable solution is $2/\omega$, where ω is the highest natural undamped frequency. This is identical to the stability limit on the BR-1 procedure.

Introducting that part of $\{F\}$ due to $\dot{w}$ given by Eq. 10a into Eq. 2 results in the modified equations of motion

$$[M]\{\ddot{q}^*\} + [D]\{\dot{q}^*\} = \{C\} \tag{16}$$

Replacing $\{\ddot{q}^*\}$ with the conventional central difference approximation

$$\{\ddot{q}^*\}_{t_i} = \left(\{q^*\}_{t_{i+1}} - 2\{q^*\}_{t_i} + \{q^*\}_{t_{i+1}}\right) \Big/ (\Delta t)^2 \tag{17a}$$

is equivalent to obtaining $\{\ddot{q}^*\}_{t_i}$ from Eq. 11 with $\{\dot{q}_I^*\}$ not considered, i.e.

$$\{\ddot{q}^*\}_{t_i} = \left(\{\Delta q^*\}_{t_{i+1}} - \{\Delta q^*\}_{t_i}\right) \Big/ (\Delta t)^2 \tag{17b}$$

according to Eq. 12. Substituting Eq. 15 for $\{\dot{q}^*\}_{t_i}$ and Eq. 17b for $\{\ddot{q}^*\}_{t_i}$ into Eq. 16 leads to

$$\{\Delta q^*\}_{t_{i+1}} = [M + D(\Delta t/2)]^{-1}\left([M - D(\Delta t/2)]\{\Delta q^*\}_{t_i} + \{C\}_{t_i}\right) \tag{18}$$

which is equivalent to $\{\Delta q^*\}_{t_{i+1}}$ given by Eqs. 11 and 13 when D is a null matrix and $\{\dot{q}_I^*\}$ is not considered.

The mass matrix [M] is developed in BR-1 using the lumped mass approach and is given by (Eq. A-97, Ref. 1)

$$[M] = \begin{bmatrix} [M_1] & & & \\ & [M_2] & & \\ & & \ddots & 0 \\ & 0 & & \ddots \\ & & & [M_R] \end{bmatrix} \tag{19a}$$

where $[M]_r$ is a 6x6 matrix given by

$$[M]_r = \sum_{n_r} [J_n]^T [m_{n_\alpha}] [J_n] \quad \alpha \longrightarrow r \tag{19b}$$

and $[m_{n_\alpha}]$ is a diagonal matrix of the lumped mass at the α node of the nth element. Comparing Eq. 10b with Eq. 19a reveals that the two matrices $[M + D(\Delta t/2)]$ and $[M - D(\Delta t/2)]$ occupy the same nonzero 6x6 locations as the original matrix M. Thus, the same procedure used in BR-1 to compute $[M]^{-1}$ can be used to compute $[M + D(\Delta t/2)]^{-1}$. Its only necessary to modify the elements of $[M]_r$ by the addition of the damping matrix $[D]_r$ given by Eq. 10c. The other necessary change is the addition of the Matrix $[M - D(\Delta t/2)]$ as a product with $\{\Delta q^*\}_{t_i}$.

Thus since

$$\underline{M}^{-1} = \begin{bmatrix} [M_1]^{-1} & & & \\ & [M_2]^{-1} & & C \\ & & \ddots & \\ & 0 & & \ddots \\ & & & & [M_R]^{-1} \end{bmatrix} \tag{20}$$

Eq. 18 can be expressed in the form

$$\{\Delta q^*\}_{rt_{i+1}} = [M_r + D_r\,(\Delta t/2)]^{-1} \left([M_r - D_r\,(\Delta t/2)]\,\{\Delta q^*\}_{rt_i} + \{C\}_{rt_i} \right), \qquad r = 1, 2, \ldots R \tag{21}$$

C. Program Changes and Modification Logic

The following routines of the IBM version of BR-1 have been modified for BR-1HR: MAIN, MEMBER, MTERM, QPLATE, STØRE, DELTT, DEFLX, REVIV1 and REVIV2. Two new subroutines were created: DPMASS and ADDAMP. The core size was increased from 250k bytes to 290k bytes.

The flow of the logic of the modifications is as follows:

1. Compute $[M]_r$ in STØRE (no change)
2. Compute $[D]_r$ in STØRE
3. Compute $[M]_r^{-1}$ in MTERM (no change)
4. Compute maximum time interval for numerical stability in DELTT based on [M] (no change)
5. Take the inverse of $[M]_r^{-1}$ to get $[M]_r$ in DPMASS using INVS
6. Compute $[M_r + D_r\ (\Delta t/2)]$ and $[M_r - D_r\ (\Delta t/2)]$ in DPMASS
7. Compute $[M_r + D_r\ (\Delta t/2)]^{-1}$ in DPMASS using INVS
8. Compute $[M_r + D_r\ (\Delta t/2)]^{-1}\ [M_r - D_r\ (\Delta t/2)]$ in DPMASS
9. Compute $[M_r + D_r\ (\Delta t/\Delta)]^{-1}\ [M_r - D_r\ (\Delta t/\Delta)]\ \{\Delta q^*\}_{t_i}$ in ADDAMP
10. Compute $\{\Delta q^*\}_{t_{in}}$ using Eq. 21 in DEFLX (no change)

The phrase "no change" means that the original procedure was used. When no damping is considered the modifications and additions are bypassed.

III. USER'S INSTRUCTIONS FOR BR-1HR

The instructions for the use of the BR-1 code are given in Ref. 2. All of the instructions contained in that volume also apply to the modified program BR-1HR. The time step for numerical stability of BR-1HR is identical to that of BR-1. The additional instructions required to use BR-1HR are as follows:

1. Problem Control Card (page 4, Ref. 2)

   IHR (I5, Col. 66-70) (follows IREV) - IHR = 0, no fluid is involved; the original BR-1 code is used. IHR = 1, fluid is involved, the modifications are used.

2. Rectangular Panel Card (page 8, Ref. 2)

   RHØCF (E8.4, Col. 55-62) (between RHØ and Table CØDE) - RHØCF is the product of γ_f, the fluid specific weight, and c, the sonic velocity of the fluid. The units of $\gamma_f c$ are lb_f -$in.^{-2}$ - $sec.^{-1}$ If the panel is not in contact with the fluid, RHØCF = 0.

IV. SAMPLE PROBLEM

A simply supported square plate is subjected to a step pressure load of the form

$$p = o \qquad t = o$$

$$p = P \sin \frac{\pi x}{a} \sin \frac{\pi y}{a} \qquad t \geq o \tag{22}$$

Due to symmetry, only one quarter of the plate is considered: The parameters of the problem are:

$E = 10.4 \times 10^6$ psi - Young's modulus

$\gamma = 0.0965$ lb/in.^{3} - specific weight of the plate

$\upsilon = 1/3$ - Poisson's ratio

$h = 0.1$ in. - thickness

$a = 20$ in. - length and width

$P = 0.01$ lb/in.^{2}

The load is sufficiently small such that the nonlinear effects are negligible. The plate is modeled with four elements as shown in Fig. 1.

The equation governing the damped motion of the plate corresponding to Eq. 16 is

$$D\nabla^4 w + \frac{\gamma h}{g} \ddot{w} + c\dot{w} = P \sin \frac{\pi x}{a} \sin \frac{\pi y}{a} \tag{23}$$

where

$$D = \frac{Eh^3}{12(1-\nu^2)}, \quad \nabla^4 = \frac{\partial^4}{\partial x^4} + 2\frac{\partial^4}{\partial x^2 \partial y^2} + \frac{\partial^4}{\partial y^4}$$

and g is the local acceleration due to gravity. The solution to Eq. 23 is

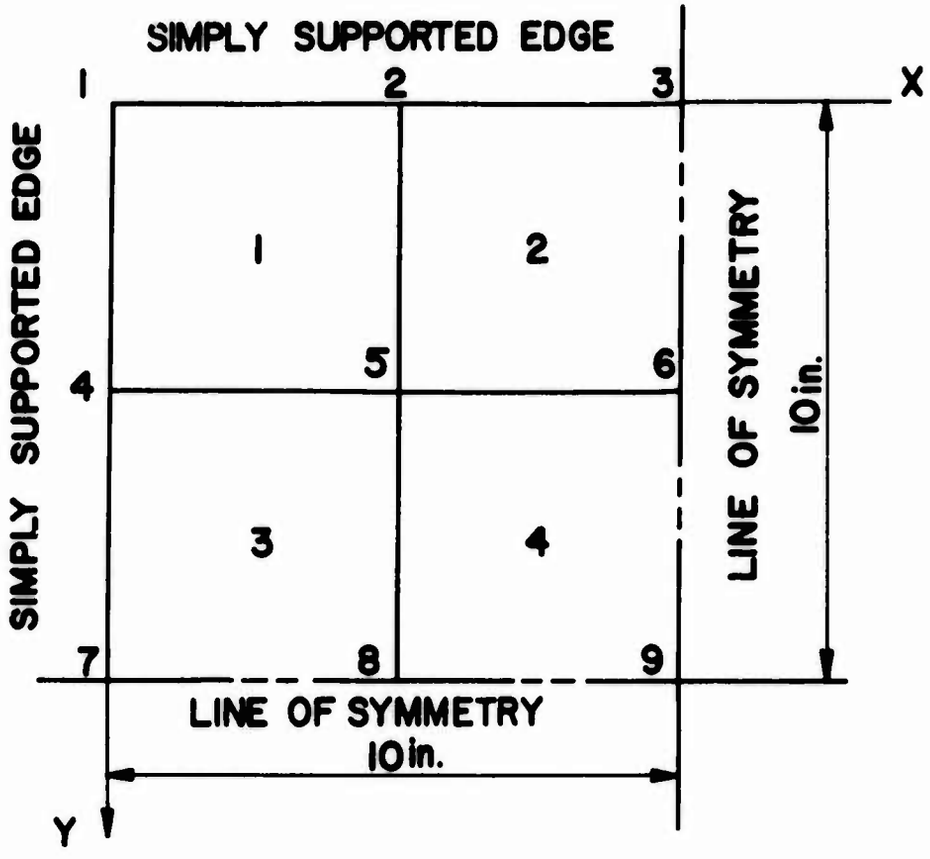

$E = 10.4 \times 10^6$ psi $\qquad \nu = 1/3$

$\gamma = 0.0965$ lb/in^3 $\qquad h = 0.1$ in.

FIGURE 1. SAMPLE PROBLEM

$$w = w_{st} \{1 - e^{-\zeta\omega t} \cos (\sqrt{1 - \zeta^2}\,\omega t + \varphi) / \cos \varphi\} \qquad (24)$$

where

$$\tan \varphi = - \zeta / \sqrt{1 - \zeta^2}$$

$$w_{st} = \frac{a^4 P}{4D\pi^4} \sin \frac{\pi x}{a} \sin \frac{\pi y}{a}$$

$$\zeta = \frac{\rho c g}{2\gamma h}$$

$$\omega = \frac{2\pi^2}{a^2} \sqrt{\frac{Dg}{h\gamma}}$$

when the plate is initially at rest. The displacement at the center of the plate given by Eq. 24 is plotted in Figures 2, 3, and 4 as a function of time for ζ = 0, 0.666 and 270 corresponding to zero damping, less than critical damping and very heavy damping respectively. The corresponding values of $g\rho c$ for the fluid are 0, 4, and 1620 lb_f /(in^2-sec). Also plotted in Figs. 2-4 are the results from BR-1HR. The input data sheets and the print of the input data are given in Fig. 5. The execution time on the IBM 360/67, FORTRAN IV - Level H, was 8 min. and 26 sec. for 200 time steps with ζ = 270. The run with damping not considered took essentially the same length of time.

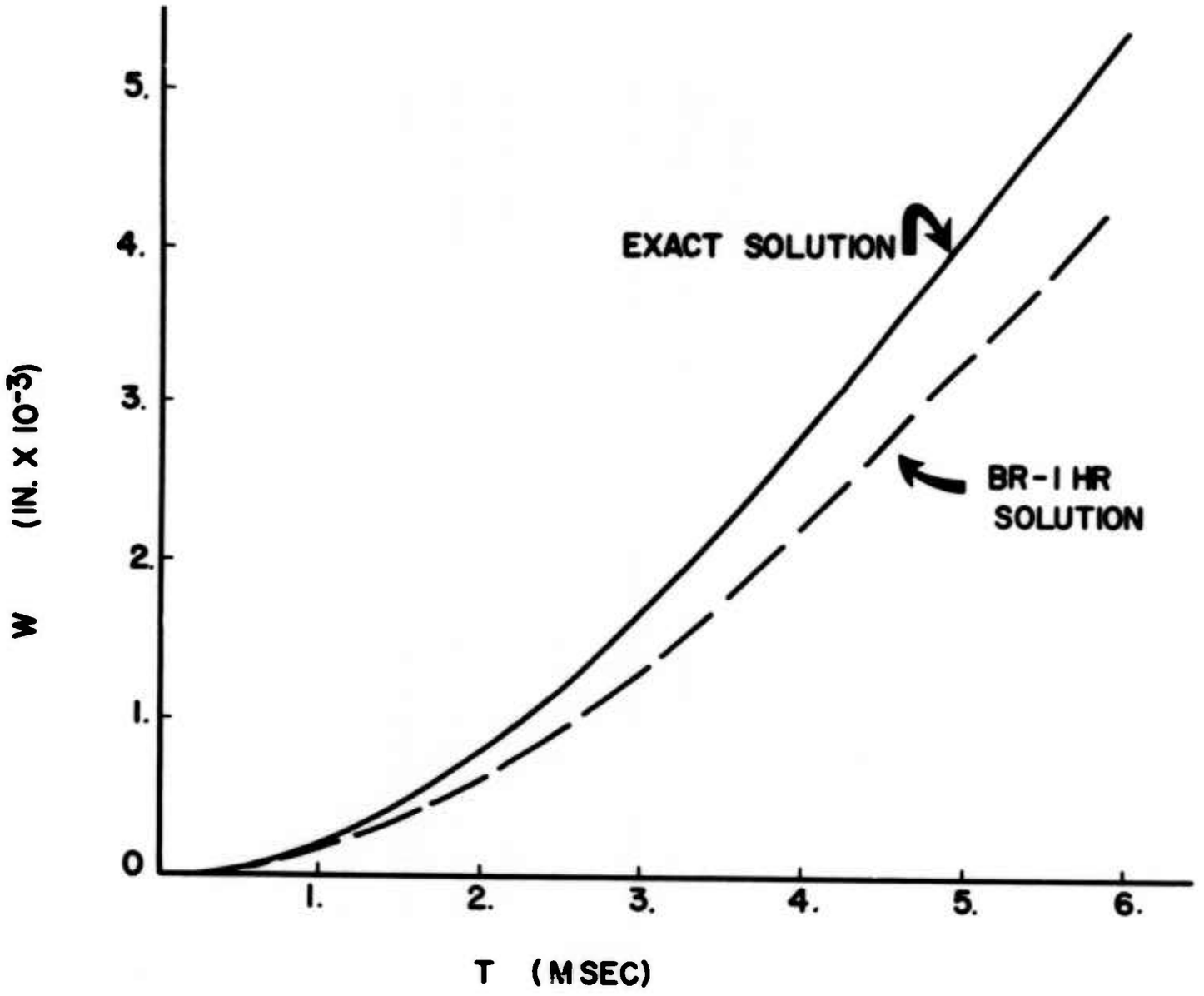

FIGURE 2. TRANSVERSE DISPLACEMENT AT NODE 9 VERSUS TIME, $f = 0$ (NO DAMPING)

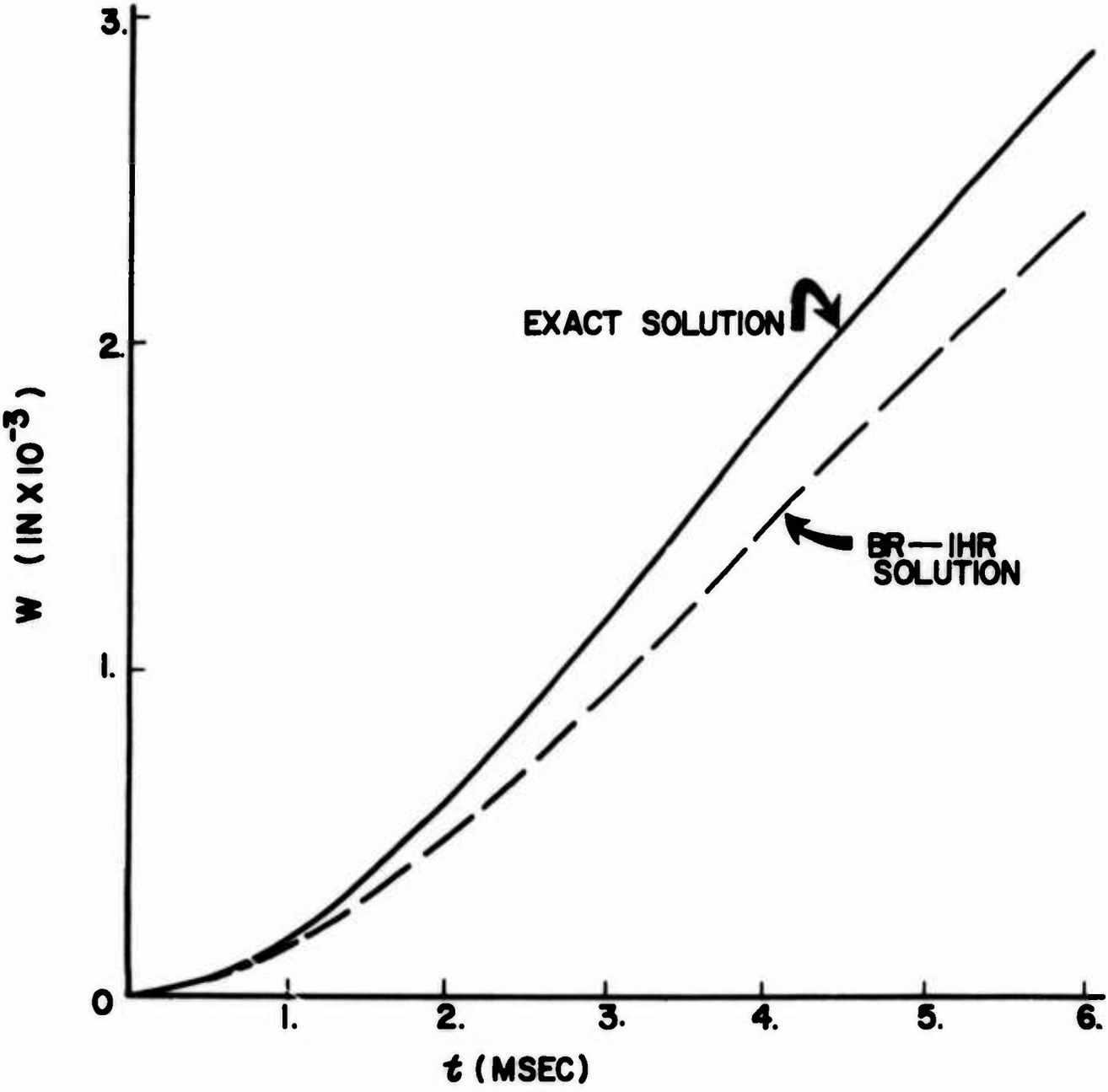

FIGURE 3. TRANSVERSE DISPLACEMENT AT NODE 9 VERSUS TIME, $\gamma = 0.666$

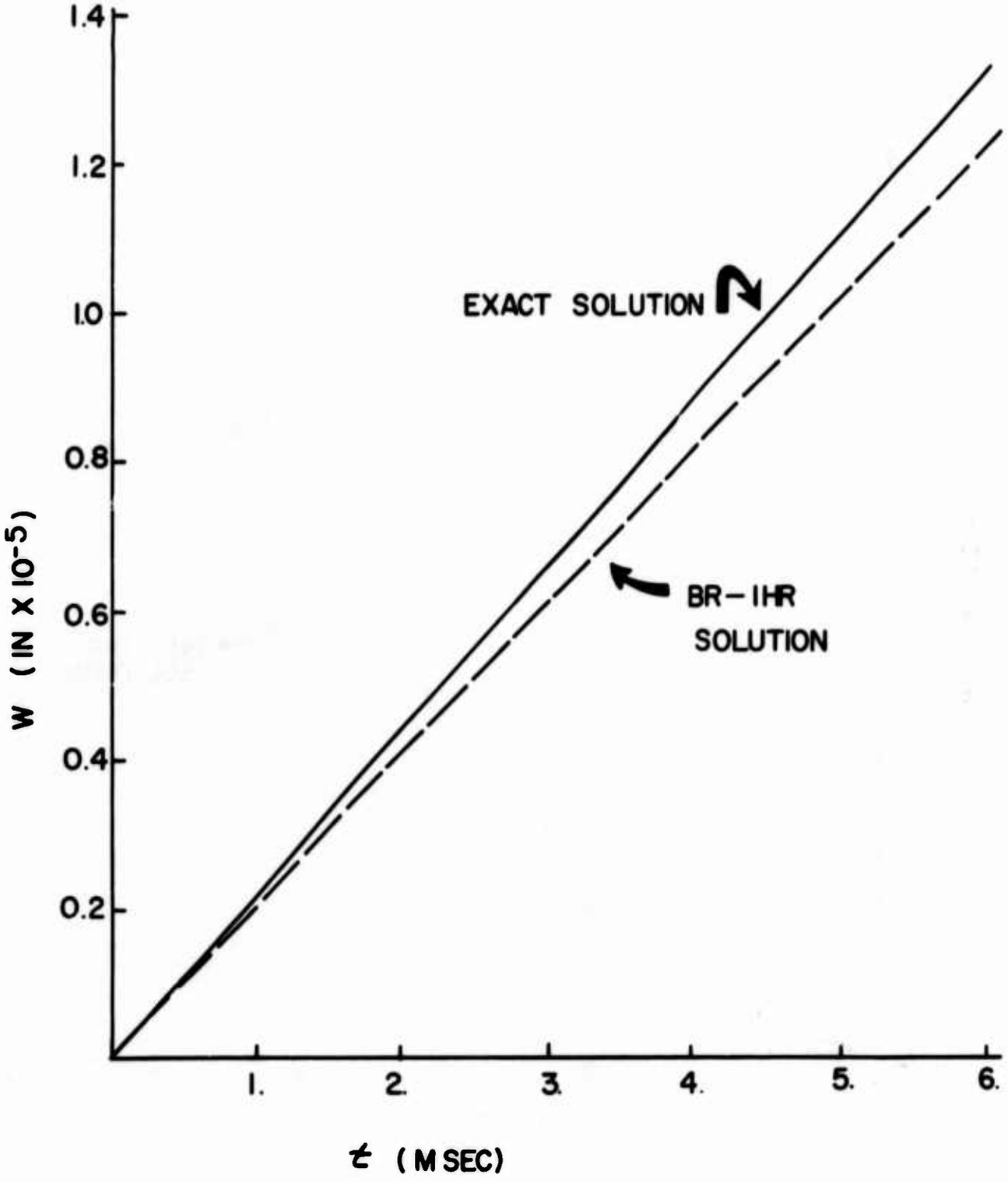

FIGURE 4. TRANSVERSE DISPLACEMENT AT NODE 9 VERSUS TIME, $\mathcal{J} = 270$

PROGRAMMER: R E BALL

PROGRAM: BR-1HR, SAMPLE PROBLEM

PAGE 1 OF 1

SPECIAL INSTRUCTIONS

CARD PUNCH OPERATOR

DATE COMPLETED

GENERAL PURPOSE CODING FORM

0 = ZERO 1 = ONE 2 = TWO
Ø = ALPHA O I = ALPHA I Z = ALPHA Z

```
A TEST CASE FOR THE H-R' VERSION OF BR-1 (BR-1HR) WITH DAMPING, RHO*C=1620
9  0  4  37  50  1  0  80  0  2  5  0  9  1
1  2  5  4  10.4  .1  .3333  .0965  1620.  1  1
2  3  6  5  10.4  .1  .3333  .0965  1620.  1  2
4  5  8  7  10.4  .1  .3333  .0965  1620.  1  3
5  6  9  8  10.4  .1  .3333  .0965  1620.  1  4
1  0.  0.  0.  2  5.  0.  0.
3  10.  0.  0.  4  0.  5.  0.
5  5.  5.  5.  6  10.  5.  0.
7  0.  10.  0.  8  5.  10.  0.
9  10.  10.  9.
1  1  1  2  1  3  1  4  1  6  2  1  2  2  2  3  2  5  2  6
3  1  3  2  3  3  3  5  3  6  4  1  4  2  4  3  4  4  4  6
6  1  6  5  6  6  7  1  7  2  7  3  7  4  7  6  8  2  8  4
8  6  9  1  9  2  9  4  9  5  9  6  5  6
1  1  0  3  0  0  .95
10.4E+6  1.
0.  0  0  4
1  .001464  2  .00  3535  3  .003535  4  .008535
```

EIGHTY COLUMN CODING SHEET 12ND NPS 5220/1 (Rev. 3/74) ★ GPO 788-888

Figure 5. Input Data Sheet

V. SUMMARY AND CONCLUSIONS

The finite element digital computer code BR-1 developed by the Northrop Corporation for predicting the effects of internal air blast on typical combat aircraft skin-rib-stringer structures has been modified to include the effect of compressible fluid-structure interaction. The fluid-structure interaction is approximated by the piston theory wherein the effect of the fluid upon the structure is accounted for by introducing damping to the equations of motion of the structure. The modified code is called BR-1HR. This code, in conjunction with the NWC code for predicting hydraulic ram pressures, can be used to predict the structural response of aircraft fuel tanks subjected to penetrating bullets and fragments.

All of the features of BR-1 exist in BR-1HR, and only two additional numbers are required for the input data. The modified code is operational on the IBM 360/67 in FORTRAN IV, level H, and requires 290K bytes of storage. A sample problem was executed to demonstrate the validity of the modified code for zero damping, less than critical damping, and very heavy damping.

VI. REFERENCES

1. Brass, J., Yamane, J. R., and Jacobson, M. J., "Effects of Internal Blast on Combat Aircraft Structure, Volume I. Engineer's Manual," Air Force Flight Dynamics Laboratory, Tech. Rpt. AFFDL-TR-73-136, Vol. I, Jan. 1974.

2. Brass, J., Yamane, J. R., and Jacobson, M. J., "Effects of Internal Blast on Combat Aircraft Structure, Volume II. User's and Programmer's Manual," Air Force Flight Dynamics Laboratory Tech. Rpt. AFFDL-TR-73-136, Vol. II, Jan. 1974.

3. Lundstrom, E., "Fluid Dynamic Analysis of Hydraulic Ram," Naval Weapons Center, NWC TP 5227, July 1971.

4. Bedrosian, B. and DiMaggio, F. L., "Acoustic Approximations in Fluid-Shell Interactions," J. Eng. Mech. Div., ASCE, Vol. 98, No. EM3, pp 731-742, June 1972.

5. Klosner, J. M., "Inadequacies of Piston Theory in Fluid-Shell Interactions," J. Eng. Mech. Div., ASCE, Vol. 96, No. EM2, pp 143-159, April, 1970.

6. Fuhs, A. E., Ball, R. E., and Power, H. L., "FY 73 Hydraulic Ram Studies," Naval Postgraduate School, NPS-57Fu74021, Feb. 1974.

7. Lundstrom, E., "Method of Hydraulic Ram Fluid Structures Analysis-An Outline," Naval Weapons Center Working Paper, China Lake, CA.

APPENDIX - A STUDY OF THE ACCURACY AND STABILITY OF SEVERAL NUMERICAL INTEGRATION SCHEMES FOR THE TRANSIENT RESPONSE OF HEAVILY DAMPED STRUCTURES

Many studies have been made of the accuracy and stability of numerical integration schemes for the equations of motion of structural systems. However, most of these studies concentrate on the response of undamped, or lightly damped, systems. Of interest here is the response of both lightly damped and heavily damped systems since both kinds of damping can occur when a structure is vibrating in contact with a compressible fluid (6).

The equations of motion of the system under consideration are given in matrix form by Eq. 16. Three different finite difference schemes for the numerical solution of these equations are considered here. Only explicit, non-iterative schemes are considered due to the fact that the BR-1 code uses an explicit solution procedure. Two of the three schemes are based upon a two variable approach using $\{q^*\}$ and $\{v^*\}$, where

$$\{\dot{q}^*\} = \{v^*\} \tag{B-1}$$

Thus, Eq. 16 can be given in the form

$$\{\dot{v}^*\} = [M]^{-1} (\{C\} - [D] \{v^*\}) \tag{B-2}$$

First Scheme

Substituting the first order approximations for $\{\dot{v}^*\}$ and $\{\dot{q}^*\}$

$$\{\dot{v}^*\}_{t_i} = (\{v^*\}_{t_{i+1}} - \{v^*\}_{t_i}) / (\Delta t) \tag{B-3a}$$

$$\{\dot{q}^*\}_{t_{i+1}} = (\{q^*\}_{t_{i+1}} - \{q^*\}_{t_i})/(\Delta t) = \{\Delta q^*\}_{t_i} /(\Delta t) \qquad \text{(B-3b)}$$

into Eqs. B-1 and B-2 leads to

$$\{v^*\}_{t_{i+1}} = [I - M^{-1}D\ (\Delta t)]\ \{v^*\}_{t_i} + (\Delta t)\ [M]^{-1}\ \{C\}_{t_i} \qquad \text{(B-4a)}$$

$$\{\Delta q\}_{t_{i+1}} = \Delta t\ \{v^*\}_{t_{i+1}} \qquad \text{(B-4b)}$$

Eliminating $\{v^*\}$ from Eqs. B-4 results in

$$\{\Delta q^*\}_{t_{i+1}} = [I - M^{-1}D\ (\Delta t)]\ \{\Delta q^*\}_{t_i} + (\Delta t)^2\ [M]^{-1}\ \{C\} \qquad \text{(B-5)}$$

This is identical to the scheme used in BR-1 when damping is not considered. It is also equivalent to the scheme where the acceleration $\{\ddot{q}^*\}$ is approximated by the conventional central difference approximation, Eq. 17a. The two variable approach given by Eqs. B-4 may be more desirable than Eq. B-5 due to roundoff error considerations, i.e. $(\Delta t)^2$ in Eq. B-5 is a very small number.

Second Scheme

The second scheme uses Eq. B-4a and the simple forward Euler approximation for $\{v^*\}$ in Eq. B-1

$$\{\Delta q^*\}_{t_{i+1}} = (\Delta t)\ \{v^*\}_{t_i} \qquad \text{(B-6)}$$

in place of the backward approximation of Eq. B-4b. The solution procedure is to compute $\{v^*\}_{t_{i+1}}$ using Eq. B-4a and $\{\Delta q^*\}_{t_{i+1}}$ using Eq. B-6.

Third Scheme

The third scheme uses the conventional central difference approxi-

mations for both $\{\dot{q}^*\}$ and $\{\ddot{q}^*\}$, i.e. Eqs. 15 and 17a. This gives Eq. 18, reproduced here for convenience

$$\{\Delta q^*\}_{t_{i+1}} = [M + D\,(\Delta t/2)]^{-1}\,([M - D\,(\Delta t/2)]\,\{\Delta q^*\}_{t_i} + (\Delta t)^2\,\{C\}_{t_i}) \quad \text{(B-7)}$$

This scheme is also identical to the BR-1 scheme when damping is not considered. A two variable version of this scheme is

$$\{\Delta v^*\}_{t_{i+1}} = [M + D\,(\Delta t/2)]\,([M - D\,(\Delta t/2)]\,\{\Delta v^*\}_{t_i} + (\Delta t)\,\{C\}_{t_i}) \quad \text{(B-8a)}$$

and

$$\{\Delta q^*\}_{t_{i+1}} = (\Delta t)\,\{\Delta v^*\}_{t_{i+1}} \quad \text{(B-8b)}$$

This may have smaller roundoff error than Eq. B-7 since $(\Delta t)^2$ has been eliminated.

The Single Degree of Freedom, Damped Oscillator

The equation for the free vibrations of the single degree of freedom, damped oscillator is

$$m\ddot{q} + d\dot{q} + hq = 0 \quad \text{(B-9)}$$

Applying the three schemes described above to Eq. B-9 leads to

$$q_{t_{i+1}} - (2 - 2\zeta\bar{\omega} - \bar{\omega}^2)\,q_{t_i} + (1 - 2\zeta\bar{\omega})q_{t_{i-1}} = 0 \quad \text{(B-10a)}$$

$$\begin{bmatrix} 1 & 0 \\ 0 & 1 \end{bmatrix} \begin{Bmatrix} (\Delta t)v \\ q \end{Bmatrix}_{t_{i+1}} - \begin{bmatrix} 1 - 2\zeta\bar{\omega} & -\bar{\omega}^2 \\ 1 & 1 \end{bmatrix} \begin{Bmatrix} (\Delta t)v \\ q \end{Bmatrix}_{t_i} = 0 \quad \text{(B-10b)}$$

$$(1 + \zeta\bar{\omega})q_{t_{i+1}} - (2 - \bar{\omega}^2)q_{t_i} + (1 - \zeta\bar{\omega})q_{t_{i-1}} = 0 \quad \text{(B-10c)}$$

where

$$\bar{\omega} = (\Delta t)\omega \qquad \omega = \sqrt{h/m} \qquad \zeta = d/(2m\omega)$$

according to Eqs. B-5, B-4a and B-6, and B-7, respectively.

The solution to Eq. B-9 can be given in the form

$$q_{t_i} = A\left(e^{-\zeta\bar{\omega}}\, e^{\mp\bar{\omega}\sqrt{\zeta^2 - 1}}\right)^i = (A_c^{\lambda})^i \tag{B-11}$$

where A is an arbitrary constant and the superscript i denotes the ith power. The solution to the three difference schemes for an arbitrary set of initial conditions can be obtained by assuming

$$q_{t_i} = A\lambda^i \tag{B-12a}$$

$$(\Delta t)v_{t_i} = B\lambda^i \tag{B-12b}$$

where λ, A and B are unknown constants. Substituting Eqs. B-12 into Eqs. B-10 and solving for λ for each scheme lead to

$$\lambda_1 = 1 - \zeta\bar{\omega} - \bar{\omega}^2/2 \mp \bar{\omega}\sqrt{(\zeta + \bar{\omega}/2)^2 - 1} \tag{B-13a}$$

$$\lambda_2 = 1 - \zeta\bar{\omega} \mp \bar{\omega}\sqrt{\zeta^2 - 1} \tag{B-13b}$$

$$\lambda_3 = \left(1 - \bar{\omega}^2/2 \mp \bar{\omega}\sqrt{\zeta^2 + \bar{\omega}^2/4 - 1}\right)/(1 + \zeta\bar{\omega}) \tag{B-13c}$$

When the discriminant in Eqs. B-11 and B-13 is positive the solution consists of damped motion only. When it is negative the motion is damped and oscillatory. Thus, a zero discriminant defines the limit of the oscillatory behavior.

The accuracy of the three numerical schemes can be evaluated by comparing λ_1, λ_2 and λ_3 with λ_c for several values of ζ and $\bar{\omega}$. The values of the ratios of the numerical solution to λ_c are given in Table B-1 for ζ = 0, 0.5, 5, and 500 and $\bar{\omega}$ = 0.1. This value of $\bar{\omega}$ corresponds to a time step of 1 μ sec when ω = 100,000 rad/sec or a time step of 1 msec when ω = 100 rad/sec, etc., i.e. the solution is computed ten times over the time interval $1/\omega$ or 20π times over the undamped natural period $2\pi/\omega$. The closer the ratio in Table B-1 is to one, the closer the numerical eigenvalue is to the correct eigenvalue.

The numerical stability of each scheme can also be determined from Eqs. B-13. When $|\lambda| > 1$ the numerical solution will be unstable. The upper limit on $\bar{\omega}$ for stability can be determined for a given value of ζ by equating $|\lambda|$ to one and solving for $\bar{\omega}$. When the discriminant is positive λ = -1 is the limiting value and the negative sign in the $\mp$ applies. When the discriminant is negative $|\lambda| = \sqrt{x^2 + y^2}$ where x and y are the real and imaginary parts respectfully. The results for the limiting values of $\bar{\omega}$ for an oscillatory solution and for numerical stability are given in Table B-2.

Scheme	$\zeta = 0$	$\zeta = 0.5$	$\zeta = 5$	$\zeta = 500$
λ_1/λ_c	$0.999999 \mp i$ 0.000042	$0.997322 \mp i$ 0.001542	$1.00005,$ 0.000002	$1.00001,$ -0.9218×10^{10}
λ_2/λ_c	$1.00499 \mp i$ 0.000333	$1.00284 \mp i$ 0.004319	$0.999949,$ 0.027185	$1.00000,$ -0.9213×10^{10}
λ_3/λ_c	$0.999999 \mp i$ 0.000042	$0.999959 \mp i$ 0.000072	$1.00000,$ 0.906095	$1.00000,$ -0.3969×10^{9}
λ_c	$0.995004 \mp i$ 0.099833	$0.947665 \mp i$ 0.082275	$0.989949,$ 0.371615	$0.999495,$ 0.2062×10^{-8}

TABLE B-1. Comparison of Numerical and Exact Solutions

Scheme	Oscillatory limit	Stability limit
λ_1	$\bar{\omega} = 2(1-\zeta)$	$\bar{\omega} = 2(\sqrt{\zeta^2+1} - \zeta)$
λ_2	$\zeta = 1$	$\bar{\omega} = 2\zeta$, $\zeta \leq 1$ $\bar{\omega} = 2\zeta - 2\sqrt{\zeta^2-1}$, $\zeta \geq 1$
λ_3	$\bar{\omega} = 2\sqrt{1-\zeta^2}$	$\bar{\omega} = 2$

TABLE B-2 Limits on $\bar{\omega}$ for an Oscillatory Solution and a Stable Solution

Note that λ_2 is unstable for any non-zero value of $\bar{\omega}$ when $\zeta=0$ and that 2 is the maximum limit on $\bar{\omega}$ for all three schemes. Also note that the limit on λ_3 is the same as that on the BR-1 routine, even with damping, and that this is the least restrictive scheme. Consequently, based upon these accuracy and stability considerations the third scheme is selected.